Enzymatic synthesis of a DNA-templated alloy nanocluster and its application in a fluorescence immunoassay

ARTICLE *in* RSC ADVANCES · JUNE 2015

Impact Factor: 3.84 · DOI: 10.1039/C5RA07509B

5 AUTHORS, INCLUDING:

Tai Ye

Wuhan University

10 PUBLICATIONS **27** CITATIONS

SEE PROFILE

Zhike He

Wuhan University

144 PUBLICATIONS **2,444** CITATIONS

SEE PROFILE

RSC Advances

PAPER

View Article Online
View Journal | View Issue

Cite this: *RSC Adv.*, 2015, **5**, 55336

Enzymatic synthesis of a DNA-templated alloy nanocluster and its application in a fluorescence immunoassay†

Tai Ye,[a] Chunying Li,[a] Chen Su,[a] Xinghu Ji[a] and Zhike He*[ab]

Received 24th April 2015
Accepted 18th June 2015

DOI: 10.1039/c5ra07509b

www.rsc.org/advances

An enzymatic synthesis strategy of a DNA-template alloy nanocluster is presented. In this strategy, alkaline phosphatase (ALP) catalysed pyrophosphate (PPi) hydrolysis broke the coordination between Cu^{2+} and PPi. The fluorescent DNA-template alloy nanoclusters were produced *in situ* through the reduction of the Cu^{2+} and Ag^{+} in the presence of single strand DNA (ss DNA). The fluorescence intensity of the alloy nanocluster was related to the concentration of ALP. This fluorescence turn-on strategy exhibited high sensitivity and selectivity for the ALP assay. Additionally, this strategy was also applied in an ALP-linked immuno-sorbent assay for a-fetoprotein (AFP) detection. Taking AFP as the model protein, it could be detected at a range from 10 ng mL^{-1} to 150 ng mL^{-1} and the detection limit was 4 ng mL^{-1} (0.042 nM). Finally, the diagnostic capability and practical application of this method was demonstrated by detecting AFP in human blood serum.

Introduction

DNA-templated metal nanoclusters (NCs) have drawn much interest because of their subnanometer size, nontoxicity and photo-stability, which make them more competitive than organic dyes or quantum dots.[1–4] Among various metallic NCs, the main advantage of DNA-templated Ag NCs is their easy functionalization with aptamers.[5] Sharma and co-workers first developed aptamer functional Ag NCs for thrombin detection based on target-induced Ag NC quenching.[6] Liu and Yang developed an aptasensor which consisted of an aptamer and Ag NCs nucleation sequence.[7,8] In the presence of the target, the nucleation sequence was released and formed Ag NCs in suit subsequently. However, biomolecular measurements in complex media such as serum are challenging due to high background signals from nonspecific binding. Several approaches have been recently reported that biological samples were pre-treated, such as multifold dilution and centrifugal filtration, which improve specificity of biomolecular detection in serum.[7,9,10] Therefore, it is highly desirable to develop a method for the protein detection in undiluted serum.

Enzyme catalysed the synthesis of nanoparticles (ECSN) provides a general strategy to integrate biocatalysis into the synthesis of nanoparticles.[11,12] Because of the high catalytic of enzyme and the unique properties of nanoparticles, ECSN has been widely used in sensing application.[13,14] Stevens and co-workers reported that the nucleation rate of silver nanocrystals on plasmonic transducers could be controlled by the concentration of glucose oxidase (GOx).[15] Rica *et al.* demonstrated that the growth kinetic of Au nanoparticle was associated with the concentration of catalase-labelled antibodies.[16,17] Nevertheless, the high sensitivity of these plasmonic enzyme-linked immunosorbent assay was dependent on the complex plasmonic structure or tedious modification process. Recently, various enzyme systems had been used to modulate the formation of fluorescent CdS quantum dots.[18–21] As ALP was the most common enzyme in labelling antibodies, this strategy was also applied to the detection of bovine serum albumin.[22] However, the toxicity of quantum dots hampered the clinical application of this technology.

Recently, Yu and co-workers developed ALP stimulated synthesis of DNA-templated copper nanoparticles through breaking the coordination between Cu^{2+} and PPi.[23] Based on the specific catalysis of ALP, which hydrolysis the PPi into orthophosphate (Pi),[24,25] an enzymatic synthesis strategy of Cu/Ag NCs was developed. In the presence of ALP, the coordination between Cu^{2+} and PPi was broken and facilitated the Cu/Ag nanocluster generation. In the contrast, the formation of Cu/Ag NCs was inhibited by the unhydrolysed PPi, resulting in the quench of Cu/Ag NCs fluorescence. This method was further applied in heterogeneous immunoassay for AFP detection. Taking advantage of the immunoassay, this protocol showed good performance in undiluted serum.

[a]*Key Laboratory of Analytical Chemistry for Biology and Medicine (Ministry of Education), College of Chemistry and Molecular Sciences, Wuhan University, Wuhan 430072, P. R. China. E-mail: zhkhe@whu.edu.cn*

[b]*Suzhou Instituite of Wuhan University, Suzhou, 215123, P. R. China. Fax: +86-27-6875-4067; Tel: +86-27-6875-6557*

† Electronic supplementary information (ESI) available. See DOI: 10.1039/c5ra07509b

Experimental

Chemical and materials

The DNA oligonucleotide (5′-CCCTTAATCCCC-3′, HPLC purified) was purchased from Sangon Biotechnology Co., Ltd. (Shanghai, China). Capture antibody, biotin antibody and antigen (AFP, prostate specific antigen, carcino-embryonic antigen) were purchased from Shanghai Linc-Bio Science Co (Shanghai, China). Silver nitrate (99+%), sodium borohydride, $NaBH_4$ (powder, 98%), thrombin, bovine serum albumin (BSA), trypsin, lysozyme, human serum albumin (HSA), and Tris(hydroxymethyl)aminomethane hydrochloride (Tris) were purchased from Sigma-Aldrich (St. Louis, MO, USA). Alkaline Phosphatase (Calf intestine) was purchased from Takara Bio, Inc. (Dalian, China). Avidin-ALP was purchase from Boster (Wuhan, China). All other chemicals not mentioned here were of analytical-reagent grade or better. 18 MΩ water purified by a Milli-Q Academic purification set (Millipore, Bedford, MA, USA) was used throughout.

Apparatus

Fluorescence spectra were obtained with a RF-5301 PC spectrophotometer (Shimadzu, Japan) equipped with a 150 W xenon lamp (Ushio Inc, Japan). Fluorescence intensity decay curves were measured on a FELIX32 system (Photon Technology International). Morphology observation of Cu/Ag NCs in Tris-HAc buffer solution (pH 7.4, 20 mM) was carried *via* transmission electron microscopy (TEM; JEM-2100 microscope) at an acceleration voltage of 200 kV. High-resolution transmission electron microscopy (HR-TEM) images were acquired with a JEM-2010 FEF at an acceleration voltage of 200 kV. All optical measurements were performed at room temperature under ambient conditions, and the fluorescence emission intensity was measured at 560 nm with excitation wavelength at 480 nm.

Detection of ALP activity by nanocluster based method

ALP of different final concentrations reacted with PPi (final concentration of 125 μM) at 37 °C for 90 min in 40 μL 20 mM Tris-HAc (pH 7.4). Cu^{2+} (final concentration of 30 μM) was then added to give a final volume of 50 μL and incubated for 10 min. After that, the ssDNA template (100 μM, 5 μL) and $AgNO_3$ (1.5 mM, 3 μL) were added into the mixture and incubated in an ice bath for 15 min. Then, reduced by the addition of $NaBH_4$ (1.5 mM, 3 μL), and the fluorescence intensity was recorded at a fixed reduction time of 60 min.

Detection of AFP by nanocluster-based immunoassay

The 96-well NUNC microplate was coated with 100 μL capture antibody solution (10 μg mL^{-1}) for overnight at 4 °C. Then the substrate was blocked with 200 μL blocking buffer solution (Tris 10 mM, NaCl 150 mM, BSA 1%, pH 8.0) for 1 h. Subsequently, a 50 μL AFP standards or samples and 10 μL biotin antibody (5 μg mL^{-1}) solution was injected. After incubation for 30 min at 37 °C, the resulting mixture was washed three times with washing buffer solution (Tris 10 mM, NaCl 150 mM, Tween 0.01%, pH 8.0). The avidin–ALP conjugate (1 : 1000) in PBS was incubated on the plate for 30 min at 37 °C. The plate was then washed three times with washing buffer solution and one time with 20 mM Tris-HAc buffer solution (pH 7.4). Then 50 μL of ALP substrate (0.1 mM PPi in 50 mM Tris-HAc buffer, pH 7.4) was added to each well and incubated for 90 min at 37 °C. After samples were drawn from the wells, Cu^{2+} (final concentration of 30 μM) was then added to give a final volume of 50 μL and incubated for 10 min. After that, the ss DNA template (100 μM, 5 μL) and $AgNO_3$ (1.5 mM, 3 μL) were added into the mixture and incubated in an ice bath for 15 min. Then, reduced by the addition of $NaBH_4$ (1.5 mM, 3 μL) and the fluorescence intensity was recorded at a fixed reduction time of 60 min.

Results and discussion

Due to the sequence and structure dependence,[26,27] DNA-template Ag NCs showed poor performance in real sample detection. In order to overcome this hurdle, we combined the enzymatic synthesis of DNA-templated alloy nanocluster with immunoassay for AFP detection. As shown in Fig. 1, in the presence of AFP, the ALP catalyzed PPi hydrolysis which broke down the coordination between Cu^{2+} and PPi. The released Cu^{2+} promoted Cu/Ag NCs formation which exhibited a strong fluorescence. In the contrast, the products showed negligible fluorescence which indicated that PPi–Cu^{2+} complex inhibited the alloy nanocluster formation.

The key component of this assay was the ALP catalysis process. Therefore, we chose ALP as the target to investigate the feasibility of this strategy (Fig. 2). In the absence of PPi, the synthesized Cu/Ag NCs showed a distinctive fluorescence intensity at 560 nm when excited at 480 nm (curve a). After Cu^{2+} was coordinated with PPi, an obvious fluorescence decreased was observed (curve b). These results indicated that PPi could strongly chelated with Cu^{2+}, which was consistent with the previous report.[23] Additionally, after incubated with ALP at 37 °C for 90 min, the fluorescence of Cu/Ag NCs was recovered (curve c).

The obtained Cu/Ag NCs were also characterized by using transmission electron microscopy (TEM). The TEM images of Cu/Ag NCs were shown in Fig. 3A. Numerous tiny clusters were visualized with a relative narrow size distribution which was consistent with the previous report.[28] The lifetime of Cu/Ag NCs

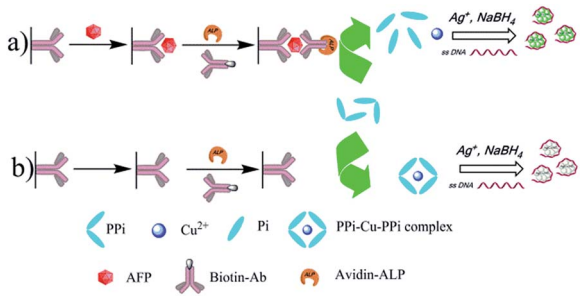

Fig. 1 Schematic representation of AFP detection system based on enzymatic synthesis of Cu/Ag nanoclusters.

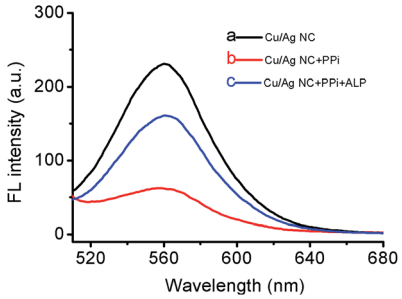

Fig. 2 Fluorescence spectra of obtained Cu/Ag NCs under different conditions: (a) in the absence of PPi, (b) 125 μM PPi (c) 125 μM PPi + 10 U L^{-1} ALP.

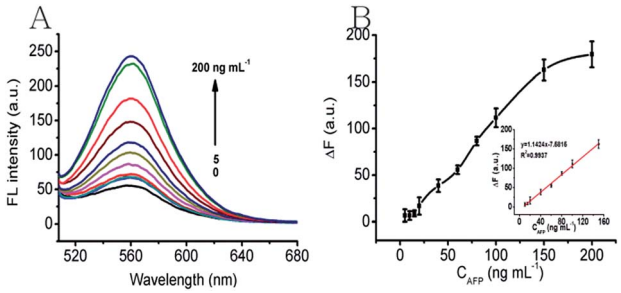

Fig. 4 (A) Fluorescence response to the different concentrations of AFP: 5, 10, 15, 20, 40, 60, 80, 100, 150, and 200 ng mL^{-1} (from bottom to top). (B) Corresponding calibration curve of the Cu/Ag NCs strategy for AFP detection. Insert: linear response at low concentrations of AFP.

and Ag NCs (Fig. 3) were investigated by time-correlated single photon counting (TCSPC) technique. The life time of Ag NCs (red curve) was 1.564 ns while the life time of the Cu/Ag NCs (black curve) was 1.737 ns. The longer excited-state lifetime suggested that the alloy nanocluster showed better photostability than that of the Ag NCs.

The optimal conditions required for the detection of ALP were evaluated. The reduction time of the Cu/Ag NCs was the key component of this strategy. The reduction time of the synthesis of the alloy cluster was examined from 0 to 120 min (Fig. S1†). After 60 min the relative fluorescence intensity reached a plateau, so 60 min was chosen as the reduction time. Additionally, we further investigated the inhibition effect of PPi on the formation of Cu/Ag NCs. As shown in Fig. S2,† the peak intensity decreased with increasing the PPi concentration in the range from 3 to 15 μM. When the concentration of PPi was higher than 15 μM, the fluorescence intensity tended to be constant. As a result, 15 μM PPi was selected as the substrate of ALP. We also investigated the influence of ALP activity under various incubation times (Fig. S3†). The results indicated that 90 min incubation time was enough to reach the maximum activity of ALP. The mechanism of the enzymatic fluorescence assay was further investigated by the enzymatic inhibition. We chose sodium orthovanadate (Na_3VO_4) as the inhibitor for ALP. When the activity of ALP was inhibited by Na_3VO_4, the hydrolysis process was blocked, which would hamper the enzymatic growth of alloy nanocluster. The fluorescence intensity of nanocluster decreased gradually with increasing the concentration of Na_3VO_4 (Fig. S6†), which indicated the activity of ALP was crucial for the enzymatic synthesis.

Under the optimal condition, the detection ability of this method was studied by testing with various concentration of the ALP (Fig. S4†). A linear dependence between the fluorescence intensity and the concentration of the ALP was obtained in the range from 0.5 to 15 U L^{-1} with a limit of detection (LOD) as low as 0.3 U L^{-1} (3σ). Table S1† shows the comparison of different detection assays for ALP. With longer incubation time, this method outweighs other methods in terms of the high sensitivity. To evaluate the selectivity of this method, four relative proteins were selected at 2 nM which was 100 fold than that of ALP as a control experiment. The result presented in Fig. S5,† showed negligible change of fluorescence intensity for the four interference proteins. Such high selectivity was because of the exclusive catalysis of ALP for PPi.

To validate the applicability of this proposal method in real sample detection, AFP was chose as a model protein for clinical heterogeneous immunoassays for detection of general cancer biomarker in human serum. As shown in Fig. 4, a linear correlation equation $y = 1.142x - 7.581$ ($R^2 = 0.993$) was obtained for AFP from 10 to 150 ng mL^{-1}, with a limit of detection (LOD) of 4 ng mL^{-1}. Although a LOD of 4 ng mL^{-1} is not very impressive compare with some recently reported methods for AFP detection due to the poor catalysis of ALP in neutral environment, this is enough for cancer diagnostics and treatment monitoring since an elevation above 400–500 ng mL^{-1} in adults is generally indicative of hepatocellular carcinoma.[29]

The selectivity of this fluorescence immunoassay was also investigated by testing three other cancer biomarkers, including thrombin, prostate specific antigen (PSA), and carcinoembryonic antigen (CEA), at 400 ng mL^{-1} which was 10-fold

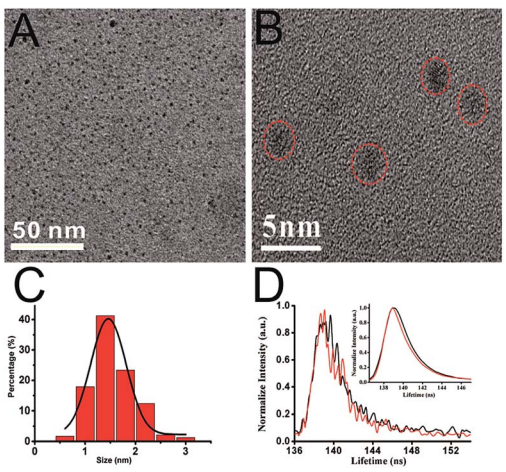

Fig. 3 The typical TEM images of the Cu/Ag NCs synthesized with PPi substrate treated with ALP (A, 0.1 U μL^{-1}) (B). High-resolution transmission electron microscopy (HR-TEM) images of Cu/Ag NCs. (C) Size distribution histogram of Cu/Ag NCs. (D) The TCSPC data for Cu/Ag NCs (black) and Ag NCs (red) (481 nm excitation, and delay time at 560 nm emissions). Insert: the fitted curve of TCSPC data.

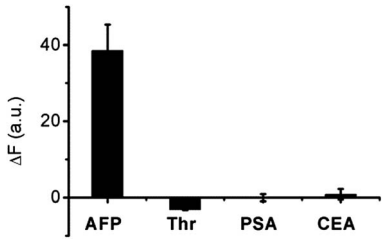

Fig. 5 Fluorescence response of fluorescence immunoassay for different proteins detection. The concentration of AFP was 40 ng mL^{-1}, and others were 400 ng mL^{-1} each.

than that of AFP. Compare with other three proteins, AFP shows remarkable change of the fluorescence intensity (Fig. 5). This result indicated good selectivity of this assay for AFP detection.

The feasibility of this assay in real sample detection was performed in human serum without pretreatment. Different concentrations of AFP were added into human serum samples. The recovery percent of AFP detected by this method in serum samples ranged from 89.8% to 105.9%, which was satisfactory for the quantitative assays performed in biological samples (Table S2†).

Conclusions

In this work, an enzymatic synthesis of Cu/Ag NCs was developed. This approach relied on the specific hydrolysis of ALP, which facilitated Cu/Ag alloy nanocluster formation. The alloy clusters showed better photo-stability and fast synthesis process than that of the Ag NCs. In additionally, this approach improved the specificity of protein detection based on the DNA-templated noble nanocluster and got rid of the interference from no-specific target protein.

Acknowledgements

We thank the Center of Analysis and Test of Wuhan University and the Center for electron microscopy Wuhan University for the use of Transmission Electron Microscopes. This work was financially supported by the National Key Scientific Program-Nanoscience and Nanotechnology (2011CB933600), Suzhou Nanotechnology Special Project (ZXG2013028) and the National Science Foundation of China (21275109 and 21205089).

Notes and references

1 A. Kumar and V. Kumar, *Chem. Rev.*, 2014, **114**, 7044–7078.
2 A. Latorre and A. Somoza, *ChemBioChem*, 2012, **13**, 951–958.
3 Z. Yuan, Y. C. Chen, H. W. Li and H. T. Chang, *Chem. Commun.*, 2014, **50**, 9800–9815.
4 P. D. Howes, R. Chandrawati and M. M. Stevens, *Science*, 2014, **346**, 1247390.
5 B. Han and E. Wang, *Anal. Bioanal. Chem.*, 2012, **402**, 129–138.
6 J. Sharma, H. C. Yeh, H. Yoo, J. H. Werner and J. S. Martinez, *Chem. Commun.*, 2011, **47**, 2294–2296.
7 Y. Xiao, Z. Wu, K. Y. Wong and Z. Liu, *Chem. Commun.*, 2014, **50**, 4849–4852.
8 J. J. Liu, X. R. Song, Y. W. Wang, A. X. Zheng, G. N. Chen and H. H. Yang, *Anal. Chim. Acta*, 2012, **749**, 70–74.
9 J. Li, X. Zhong, H. Zhang, X. C. Le and J. J. Zhu, *Anal. Chem.*, 2012, **84**, 5170–5174.
10 K. S. Park, S. S. Oh, H. T. Soh and H. G. Park, *Nanoscale*, 2014, **6**, 9977–9982.
11 I. Willner, R. Baron and B. Willner, *Biosens. Bioelectron.*, 2007, **22**, 1841–1852.
12 I. Willner, R. Baron and B. Willner, *Adv. Mater.*, 2006, **18**, 1109–1120.
13 R. de la Rica, D. Aili and M. M. Stevens, *Adv. Drug Delivery Rev.*, 2012, **64**, 967–978.
14 P. D. Howes, S. Rana and M. M. Stevens, *Chem. Soc. Rev.*, 2014, **43**, 3835–3853.
15 L. Rodríguez-Lorenzo, R. de la Rica, R. A. Álvarez-Puebla, L. M. Liz-Marzán and M. M. Stevens, *Nat. Mater.*, 2012, **11**, 604–607.
16 R. de la Rica and M. M. Stevens, *Nat. Nanotechnol.*, 2012, **7**, 821–824.
17 R. de la Rica and M. M. Stevens, *Nat. Protoc.*, 2013, **8**, 1759–1764.
18 G. Garai-Ibabe, M. Moller and V. Pavlov, *Anal. Chem.*, 2012, **84**, 8033–8037.
19 L. Saa and V. Pavlov, *Small*, 2012, **8**, 3449–3455.
20 G. Garai-Ibabe, L. Saa and V. Pavlov, *Anal. Chem.*, 2013, **85**, 5542–5546.
21 G. Garai-Ibabe, L. Saa and V. Pavlov, *Analyst*, 2014, **139**, 280–284.
22 N. Malashikhina, G. Garai-Ibabe and V. Pavlov, *Anal. Chem.*, 2013, **85**, 6866–6870.
23 L. Zhang, J. Zhao, M. Duan, H. Zhang, J. Jiang and R. Yu, *Anal. Chem.*, 2013, **85**, 3797–3801.
24 J. Deng, Q. Jiang, Y. Wang, L. Yang, P. Yu and L. Mao, *Anal. Chem.*, 2013, **85**, 9409–9415.
25 J. Deng, P. Yu, L. Yang and L. Mao, *Anal. Chem.*, 2013, **85**, 2516–2522.
26 D. Schultz and E. G. Gwinn, *Chem. Commun.*, 2012, **48**, 5748–5750.
27 Y. Teng, X. Yang, L. Han and E. Wang, *Chem.–Eur. J.*, 2014, **20**, 1111–1115.
28 L. Zhang, J. Zhu, S. Guo, T. Li, J. Li and E. Wang, *J. Am. Chem. Soc.*, 2013, **135**, 2403–2406.
29 Y. Deng, J. Nie, X. Zhang, M.-Z. Zhao, Y.-L. Zhou and X.-X. Zhang, *Analyst*, 2014, **139**, 3378–3383.